

Electronic Supplementary Information

Deep Fano resonance with strong polarization dependence in gold nanoplate–nanosphere heterodimers

Feng Qin,^{a,c} Yunhe Lai,^a Jianhua Yang,^a Ximin Cui,^a Hongge Ma,^{*c} Jianfang Wang^{*a,b} and Hai-Qing Lin^d

^aDepartment of Physics, The Chinese University of Hong Kong, Shatin, Hong Kong SAR, China. E-mail: jfwang@phy.cuhk.edu.hk

^bShenzhen Research Institute, The Chinese University of Hong Kong, Shenzhen 518057, China

^cScience and Technology on High Power Microwave Laboratory, Institute of Applied Electronics, China Academy of Engineering Physics, Mianyang 621900, China. E-mail: mahongge@caep.cn

^dBeijing Computational Science Research Center, Beijing 100193, China

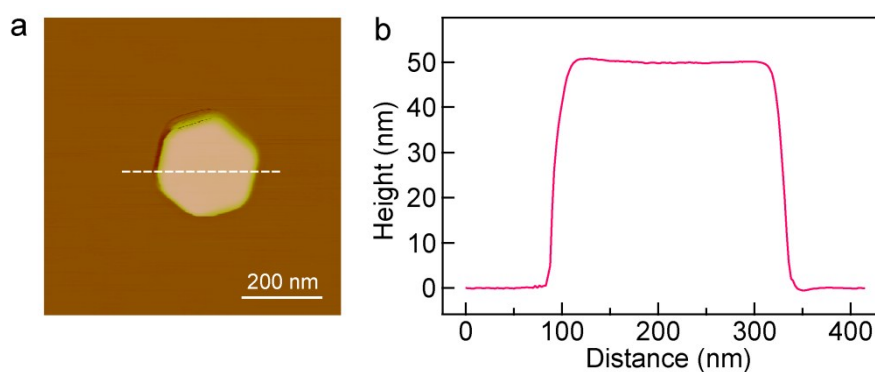


Fig. S1 AFM measurements of the Au NPLs. (a) Height image of an individual Au NPL. (b) Height profile extracted along the white dashed line indicated in (a).

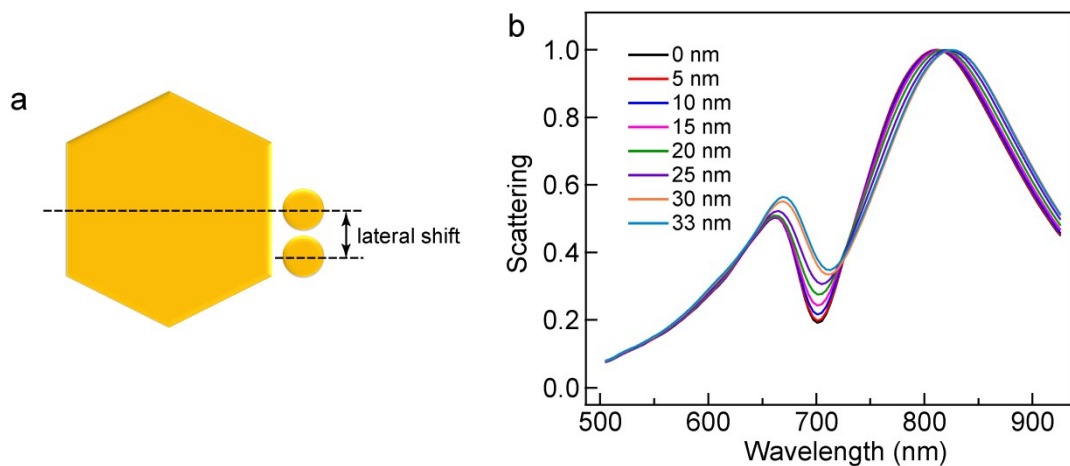


Fig. S2 FDTD simulations of the Au NPL–NS heterodimers. The Au NS is positioned on one side edge of the Au NPL. The scattering spectrum of the heterodimer was simulated as the NS was gradually shifted away from the middle of the edge of the NPL. (a) Schematic showing the lateral shift of the NS from the middle of one edge of the NPL. For the purpose of clear illustration, the size of the NS is reduced. (b) Scattering spectra simulated for the heterodimers with the NS shifted by different distances from the middle of one side edge of the NPL, as indicated by the numbers. The edge length of the Au NPL used in the simulations is 78 nm. Therefore, the lateral size of the Au NPL is 135 nm. The diameter of the Au NS is set at 50 nm.

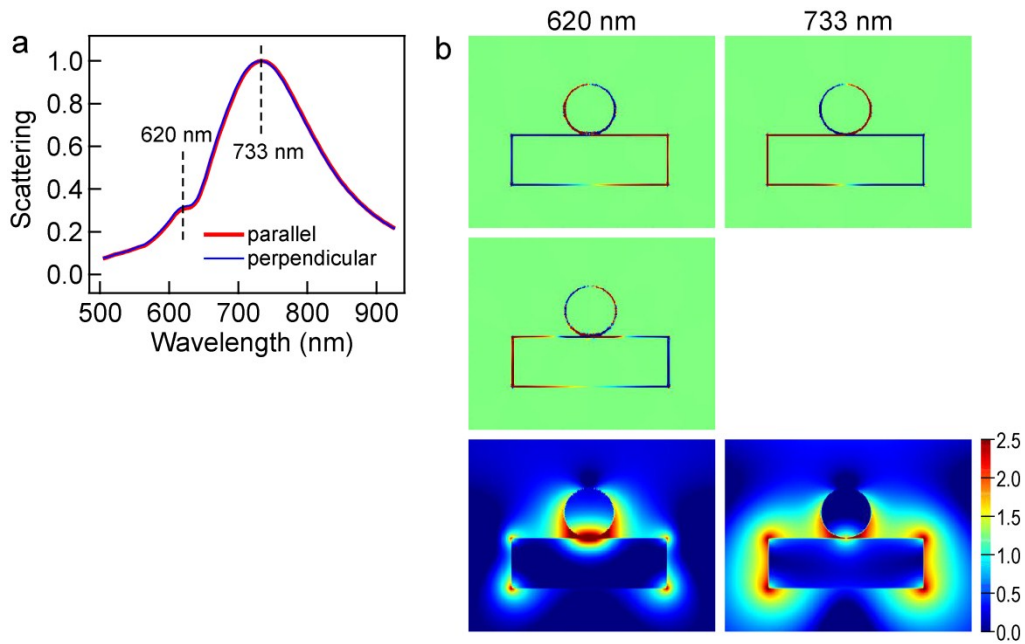


Fig. S3 FDTD simulations of the Au NPL–NS heterodimer. The NS in the heterodimer has a diameter of 50 nm and is attached on the top facet of the NPL. (a) Scattering spectra under the in-plane parallel and perpendicular excitations. (b) Charge distribution (top and middle rows) and electric field intensity enhancement (bottom row) contours at the higher-energy bump and major scattering peak wavelengths, respectively, under the in-plane parallel excitation. At the major scattering peak, the dipole of the NS is opposite to that of the NPL. At the higher-energy bump, both dipole–dipole and quadrupole–quadrupole charge contours were obtained, depending on the phase of the excitation light.

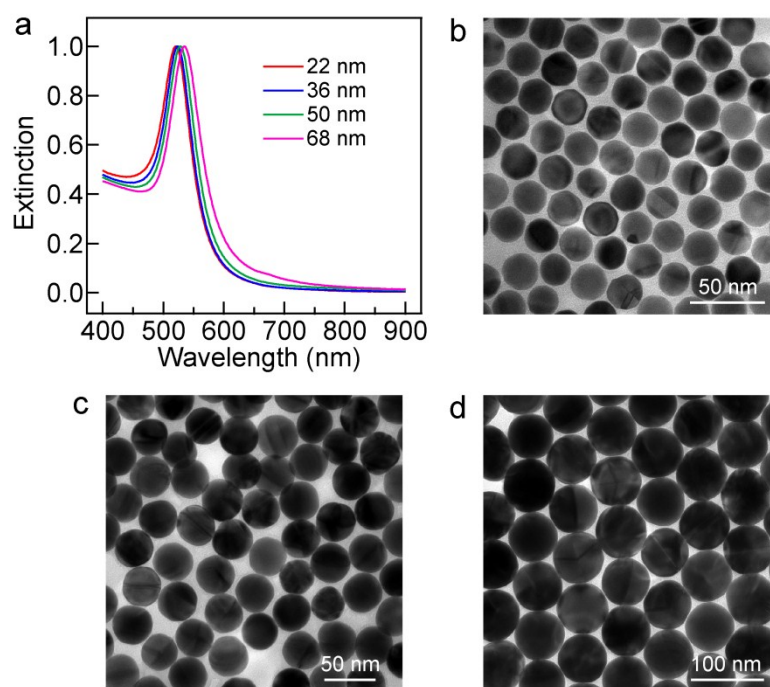


Fig. S4 Au NS samples. (a) Normalized extinction spectra of the Au NS samples. (b–d) TEM images of the three other Au NS samples. The average diameters of the three other NS samples are 22 ± 2 nm, 36 ± 3 nm, and 68 ± 4 nm, respectively.

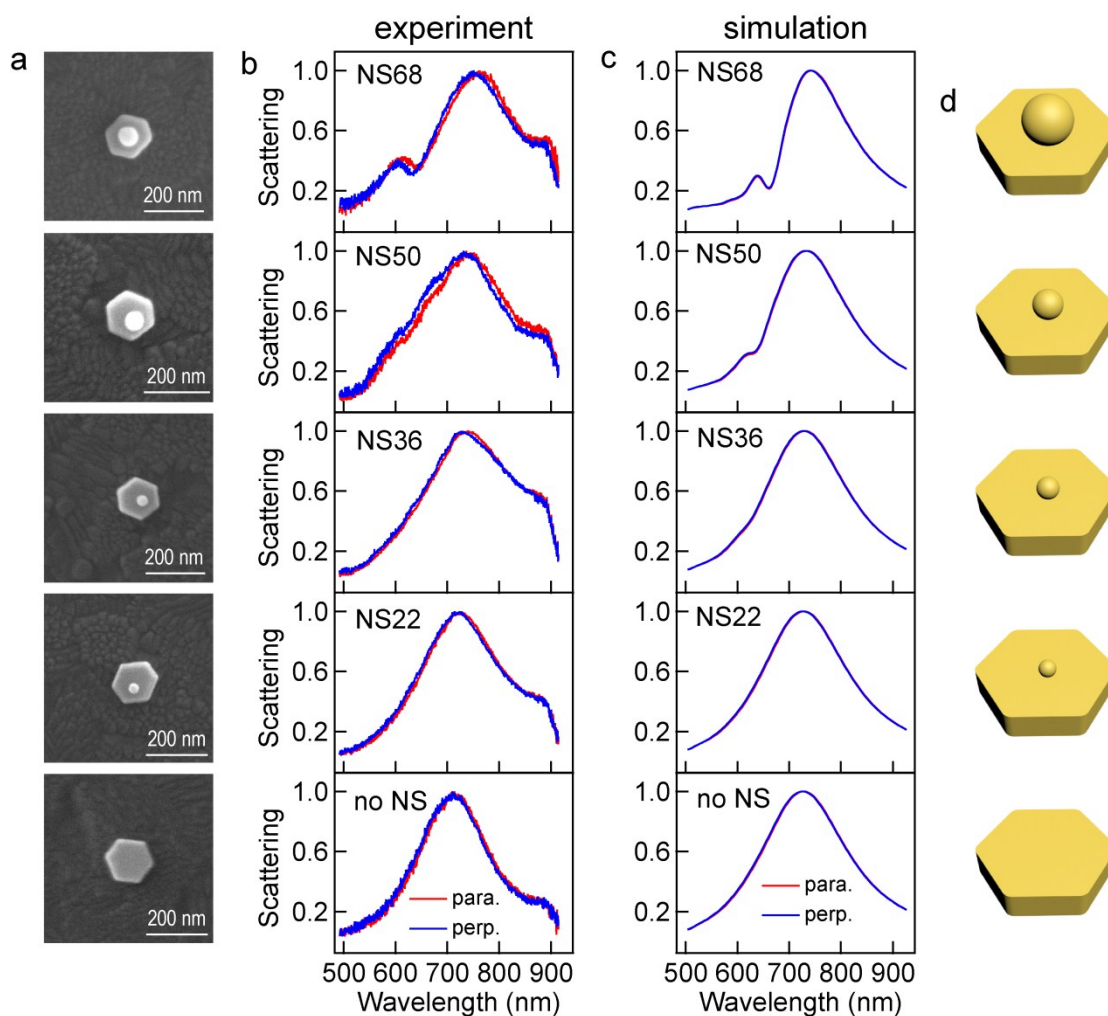


Fig. S5 Scattering spectra of the single NPL and the NPL-NS heterodimers. The NS is positioned at the top facet of the NPL. Au NSs of different diameters were used to construct the heterodimers. (a) SEM images of a representative single NPL and the heterodimers. (b, c) Measured and simulated scattering spectra, respectively. The number after ‘NS’ refers to the average diameter of the NS sample. (d) Schematic models of the single NPL and NPL-NS heterodimers.

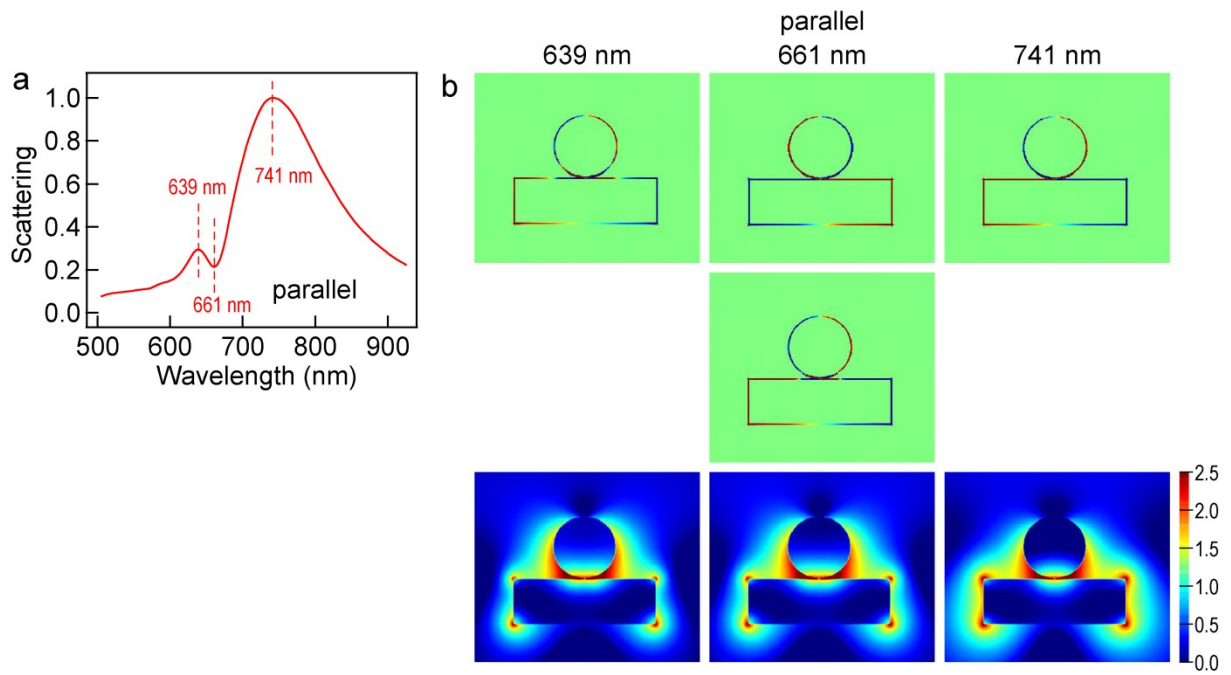


Fig. S6 FDTD simulations for the Au NPL–NS heterodimer. The NS has a diameter of 68 nm and is attached to the top facet of the NPL. (a) Scattering spectrum of the heterodimer under the in-plane parallel excitation. (b) Charge distribution (top and middle rows) and electric field intensity enhancement (bottom row) contours at the two scattering peaks and the dip. The charge distribution contour in the middle row was obtained at a phase difference of $\pi/3$ for the excitation light wave in comparison with those in the top row.

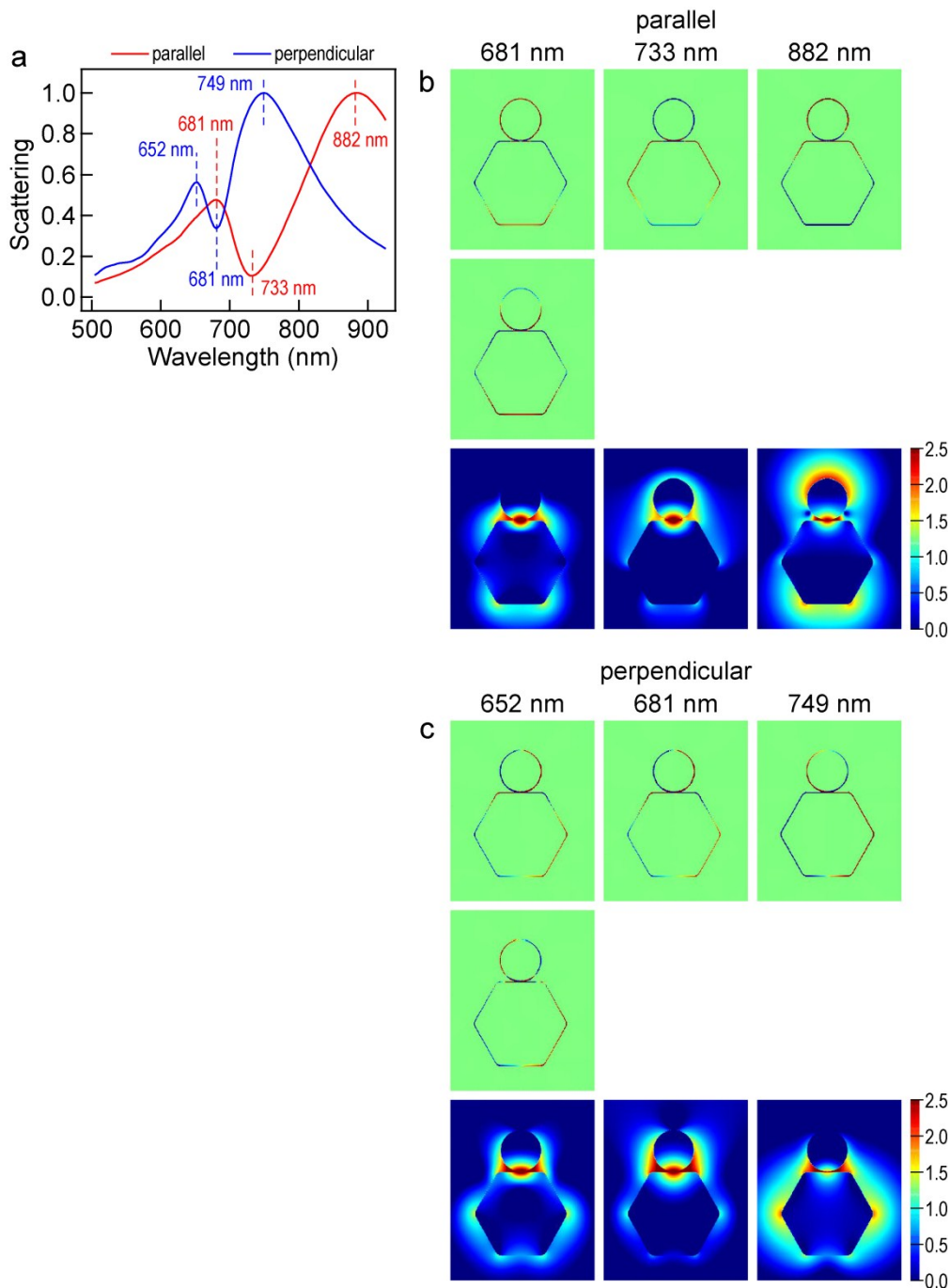


Fig. S7 FDTD simulations for the Au NPL-NS heterodimer. The NS has a diameter of 68 nm and is attached to the middle of one side edge of the NPL. (a) Scattering spectra of the heterodimer under the in-plane parallel and perpendicular excitations. (b, c) Charge distribution (top and middle rows) and electric field intensity enhancement (bottom row) contours at the two scattering peaks and the dip on the simulated spectra under the in-plane parallel and perpendicular excitations, respectively. The charge distribution contours in the middle rows in (b, c) were obtained at a phase difference of $\pi/3$ for the excitation light wave in comparison with those in the top rows.

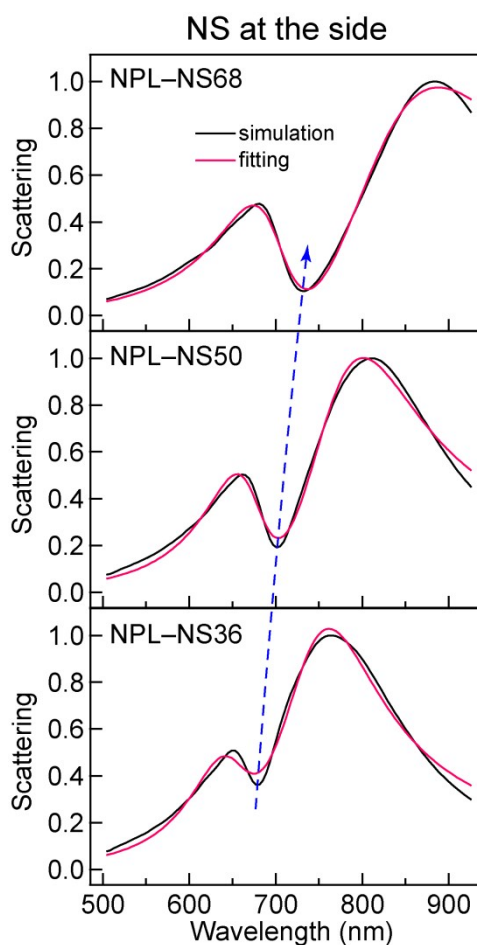


Fig. S8 Fitting of the Fano profile on the FDTD-simulated scattering spectra. The heterodimers are composed of one Au NPL and one NS that has varied diameters. The NS is positioned at the middle of one side edge of the NPL. The scattering spectra were simulated under the in-plane parallel excitation. The blue dashed line indicates the red shift in the dip position with increasing NS sizes. The coefficients of determination for the fitting are $R^2 = 0.9894$, 0.9913 and 0.9970 for the NPL-NS36, NPL-NS50 and NPL-NS68 heterodimers, respectively.

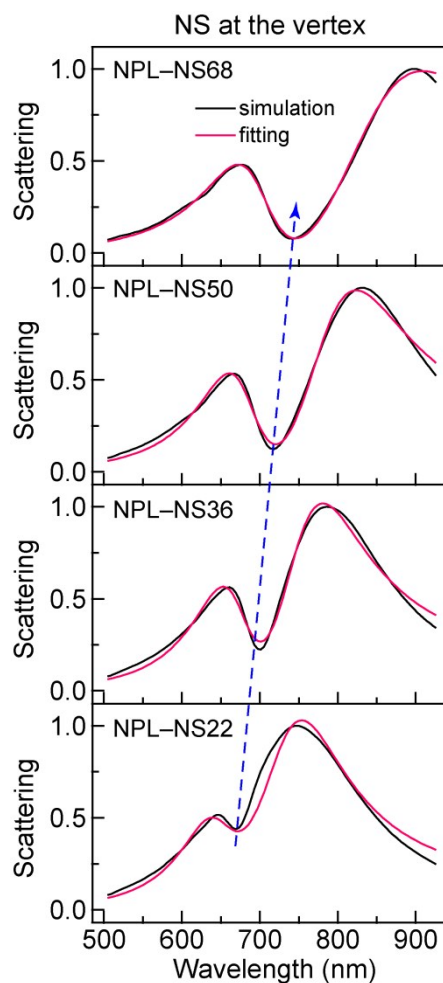


Fig. S9 Fitting of the Fano profile on the FDTD-simulated scattering spectra. The heterodimers are composed of one Au NPL and one NS that have varied diameters. The NS is positioned at one sharp vertex of the NPL. The scattering spectra were simulated under the in-plane parallel excitation. The blue dashed line indicates the red shift in the dip position with increasing NS sizes. The coefficients of determination for the fitting are $R^2 = 0.9886$, 0.9911 , 0.9925 and 0.9978 for the NPL-NS22, NPL-NS36, NPL-NS50 and NPL-NS68 heterodimers, respectively.

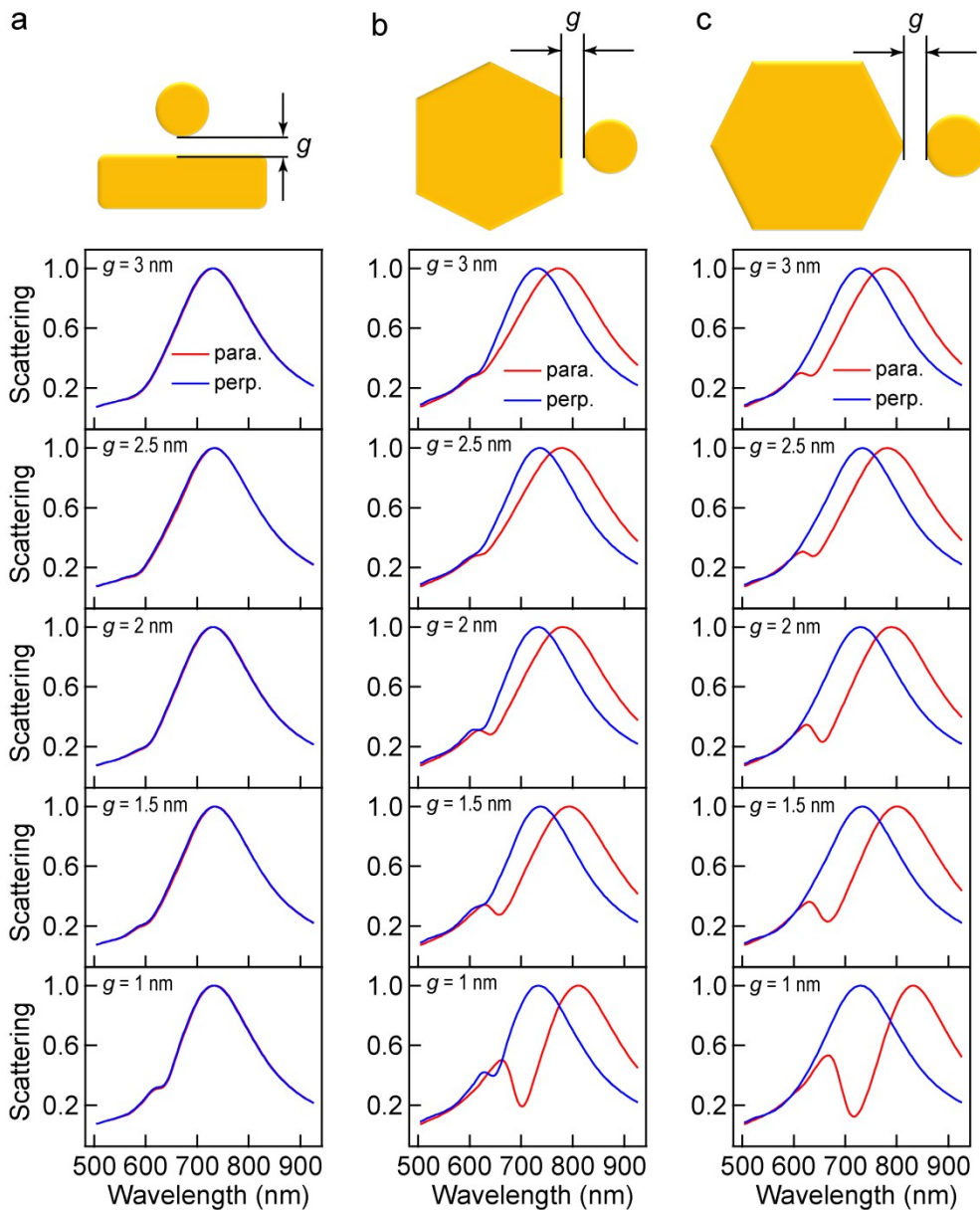


Fig. S10 Gap distance-dependent plasmon coupling in the Au NPL–NS heterodimers. The scattering spectra were obtained from FDTD simulations. (a–c) For the heterodimers with the NS positioned at the top facet, the middle of one side edge, and one sharp vertex of the NPL, respectively. On the top row are the schematic models for the three assembly configurations. The gap distance g is varied among 1, 1.5, 2, 2.5 and 3 nm. The NS has a diameter of 50 nm.

Table S1 Fitting parameters of the simulated scattering spectra shown in Fig. 5

	ω_s (eV)	γ_s (eV)	ω_a (eV)	γ_a (eV)	a	b	q
Side parallel ^a	1.59	0.18	1.83	0.12	1.41	0.31	0.53
Vertex parallel ^b	1.55	0.16	1.81	0.13	1.59	0.18	0.66

^aThe NS is positioned at the middle of one side edge. The simulation was performed under the in-plane parallel excitation. ^bThe NS is positioned at one vertex. The simulation was performed under the in-plane parallel excitation.

Table S2 Fitting parameters of the simulated scattering spectra shown in Fig. S8

	ω_s (eV)	γ_s (eV)	ω_a (eV)	γ_a (eV)	a	b	q
NS36 parallel ^a	1.65	0.17	1.89	0.12	1.36	0.59	0.47
NS50 parallel ^a	1.59	0.18	1.83	0.12	1.41	0.31	0.53
NS68 parallel ^a	1.45	0.33	1.76	0.13	1.36	0.17	0.57

^aThe NS is positioned at the middle of one side edge. The simulations were performed under the in-plane parallel excitation.

Table S3 Fitting parameters of the simulated scattering spectra shown in Fig. S9

	ω_s (eV)	γ_s (eV)	ω_a (eV)	γ_a (eV)	a	b	q
NS22 parallel ^a	1.67	0.15	1.90	0.13	1.40	0.57	0.48
NS36 parallel ^a	1.63	0.16	1.84	0.13	1.59	0.25	0.53
NS50 parallel ^a	1.55	0.16	1.81	0.13	1.59	0.18	0.66
NS68 parallel ^a	1.42	0.22	1.76	0.14	1.49	0.13	0.69

^aThe NS is positioned at one vertex. The simulations were performed under the in-plane parallel excitation.